



Fluoride Exposure Provokes Mitochondria-Mediated Apoptosis and Increases Mitophagy in Osteocytes via Increasing ROS Production

Yun Zhang¹ · Fanhe Dong¹ · Zihan Wang¹ · Bingbing Xu¹ · Tao Zhang¹ · Qiqi Wang¹ · Qiao Lin¹

Received: 14 August 2022 / Accepted: 13 October 2022 / Published online: 18 October 2022
© The Author(s), under exclusive licence to Springer Science+Business Media, LLC, part of Springer Nature 2022

Abstract

Fluoride is a persistent environmental pollutant, and its excessive intake causes skeletal and dental fluorosis. However, few studies focused on the effects of fluoride on osteocytes, making up over 95% of all bone cells. This study aimed to investigate the effect of fluoride on osteocytes *in vitro*, as well as explore the underlying mechanisms. CCK-8, LDH assay, fluorescent probes, flow cytometry, and western blotting were performed to examine cell viability, apoptosis, mitochondria changes, reactive oxygen species (ROS) and mitochondrial ROS (mtROS), and protein expressions. Results showed that sodium fluoride (NaF) exposure (4, 8 mmol/L) for 24 h inhibited the cell viability of osteocytes MLO-Y4 and promoted G0/G1 phase arrest and increased cell apoptosis. NaF treatment remarkably caused mitochondria damage, loss of MMP, ATP decrease, Cyto c release, and Bax/Bcl-2 ratio increase and elevated the activity of caspase-9 and caspase-3. Furthermore, NaF significantly upregulated the expressions of LC-3II, PINK1, and Parkin and increased autophagy flux and the accumulation of acidic vacuoles, while the p62 level was downregulated. In addition, NaF exposure triggered the production of intracellular ROS and mtROS and increased malondialdehyde (MDA); but superoxide dismutase (SOD) activity and glutathione (GSH) content were decreased. The scavenger N-acetyl-L-cysteine (NAC) significantly reversed NaF-induced apoptosis and mitophagy, suggesting that ROS is responsible for the mitochondrial-mediated apoptosis and mitophagy induced by NaF exposure. These findings provide *in vitro* evidence that apoptosis and mitophagy are cellular mechanisms for the toxic effect of fluoride on osteocytes, thereby suggesting the potential role of osteocytes in skeletal and dental fluorosis.

Keywords Fluoride · Osteocytes · Mitochondria · Apoptosis · Mitophagy · ROS

Introduction

Fluorine, widely present as fluoride in the environment, is an important trace element that can be naturally found in soil, water, and several ailments and many products used in daily life. A suitable amount of fluoride has a beneficial effect on the growth of humans and animals [1, 2]. However, excessive fluoride accumulated in humans and animals has adverse effects on various organs and systems including the kidney, liver, heart, reproductive system, nervous system, intestinal system, and endocrine system [1, 3–7]. Furthermore, excessive fluoride intake can disrupt bone

homeostasis, which causes skeletal and dental fluorosis [8–10]. Patients with skeletal fluorosis display multiple bone lesions such as osteoporosis, osteosclerosis, calcification of ligaments, and osteopenia [9, 10], which bring a lot of inconvenience to patients' life and even affect their life span. Existing data have indicated that excessive fluoride can induce abnormal proliferation and activation of osteoblasts [11, 12], leading to bone turnover disorders that may cause bone lesions of skeletal and dental fluorosis. Meanwhile, excessive fluoride triggers cellular apoptosis of osteoblasts [13, 14], which is closely associated with osteosclerosis, osteoporosis, and osteomalacia. Moreover, excessive fluoride intake promotes osteoclasts formation and bone loss [15], which increases the risk of postmenopausal osteoporosis [16]. At present, the effects of fluoride on osteoblasts and osteoclasts are well studied, but little attention to the role of osteocytes, making up over 95% of the bone cells, in skeletal and dental fluorosis.

Yun Zhang and Fanhe Dong contributed equally to this work.

✉ Yun Zhang
zhangyunbme@126.com

¹ College of Medicine, Shaoxing University, Huancheng West Road 508, Shaoxing 312000, People's Republic of China

Osteocytes, terminally differentiated cells embedded in the mineralized bone matrix, orchestrate bone remodeling by regulating the activities of osteoblasts and osteoclasts located on the bone surface [17, 18]. It has been demonstrated that ablation of osteocytes induced osteoporosis with the deterioration of bone microstructure [18]. Notably, osteocytes death by apoptosis is implicated in several key pathological factors, such as estrogen deficiency, mechanical unloading, aging, excessive glucocorticoids, and periprosthetic osteolysis [19–23], which has a link to resorption-associated bone fragility and bone destruction [20, 23]. As for the relationship between fluoride and osteocytes, Jiang et al. reported that excessive fluoride exposure significantly promoted apoptosis of osteocyte-like IDG-SW3 cells [24], which both reduces osteoblastic bone formation through sclerostin upregulation and increases osteoclastic bone resorption through receptor activator of nuclear factor- κ B ligand (RANKL) production, and ultimately leading to osteoporosis and osteoarthritis. More importantly, excessive fluoride intake also can decrease the activity of osteocytes in skeletal fluorosis of femur rats [25]. These observations suggest that osteocytes may be involved in regulating the occurrence and development of skeletal fluorosis. However, the detailed mechanism by which fluoride induces osteocytes death remains unknown.

In addition to apoptosis contributing to the toxicity of skeletal health, some recent studies have shown that mitophagy often happens to damaged mitochondria following exposure to environmental pollutants including aluminum, Cr (VI), fluoride, and carbon black [26–29]. Mitophagy, the mitochondrial selective autophagy, targets damaged mitochondria for degradation through receptor-mediated mechanisms. Its occurrence is strictly regulated by PTEN-induced putative kinase 1 (PINK1) and Parkin, which accumulates on the outer membrane of damaged mitochondria and stabilizes mitochondrial depolarization [30, 31]. Sufficient investigations have indicated that several mitochondrial proteins ubiquitinated by Parkin can bind to the phagophore by either direct binding to the autophagic adaptor protein light chain 3-II (LC3-II) or through p62, which contains an LC3 interacting domain to bind to LC3 and then promote mitophagy [31]. Mitophagy is generally believed to play protective roles under normal and disease conditions. However, emerging evidence suggests that mitophagy can become detrimental, leading to cell death under certain conditions [32, 33]. For example, mitophagy is required for the development of bone metabolic disorders such as osteoporosis and apical periodontitis. In type 2 diabetes-related osteoporosis, activation of mitophagy can inhibit osteoblasts viability through multiple components of the mitophagy pathway *in vitro* or in an animal model [32]. Also, Yang et al. reported that hypoxia could induce mitochondrial dysfunction of osteoblasts and stimulate mitophagy, resulting in bone loss in a rat model of apical periodontitis [33]. Furthermore, the level of mitophagy was increased by hypoxia in osteocytes MLO-Y4, which was alleviated by dexamethasone administration [34].

Nevertheless, whether the toxicity of fluoride to osteocytes is associated with mitophagy is still unclear.

Oxidative stress is the main pathogenic mechanism of abnormal bone metabolism and refers to the imbalance between reactive oxygen species (ROS) and antioxidant defense in the body or cells [26, 35]. ROS as “free radicals” are mainly produced in the mitochondria, which was the target organelle of ROS attack. The excessive accumulation of ROS is an inevitable side effect of mitochondrial respiration that increases the permeability of the mitochondrial membrane, resulting in mitochondria damage, mitochondrial dysfunction, and cell death [36]. Especially, the damaged mitochondria can be specifically encapsulated by autophagosomes and fused with lysosomes [31], which leads to mitophagy activation. Currently, most research has shown that environmental pollutants like aluminum could cause different degrees of oxidative damage and excessive ROS production [26], which affects mitochondria function and stimulates mitophagy, thereby exerting an obvious toxic effect on osteoblasts and bone impairment. However, the relationship between oxidative stress and mitophagy and how their interaction affects fluoride-induced osteocytes death requires further clarification.

The purpose of the present study was to investigate the effects of fluoride on the cell viability of osteocytes MLO-Y4, the generation of ROS and mitochondria ROS, cell cycle distribution, apoptosis, mitochondrial damage, and mitophagy. Our results demonstrate that fluoride exposure provokes mitochondria-mediated apoptosis and increased mitophagy in osteocytes MLO-Y4, which is mediated by increasing ROS production.

Materials and Methods

Culture of Osteocytes MLO-Y4

The murine long bone-derived osteocyte-like MLO-Y4 cells were kindly provided by Dr. Lynda Bonewald (University of Missouri-Kansas City, MO, USA). Cells were cultured in α -MEM culture media supplemented with 2.5% FBS, 2.5% CS, and 1% penicillin–streptomycin and incubated in a humidified incubator at 37 °C with 95% humidity and 5% CO₂, as we described previously [35, 37].

CCK-8 Assay

The cell viability was examined using a CCK-8 kit according to the manufacturer’s instructions. Briefly, MLO-Y4 cells (1×10^4 cells/mL) were seeded into a 96-well culture plate and treated with NaF (0, 0.25, 0.5, 2, 4, 8, 10 mmol/L) for 24 h. After removing the supernatant, CCK-8 solution (10 μ L) was added to each well of the plate. Then, cells were incubated at

37 °C for 1 h, and the OD values were measured at 450 nm using a 680 iMark microplate reader (Bio-Rad, USA).

Determination of Lactate Dehydrogenase (LDH) Release

LDH, an indicator of cell membrane permeability, measured the release of LDH using the LDH assay kit according to the manufacturer's instruction. MLO-Y4 cells were treated with NaF (0, 4, 8 mmol/L) for 24 h. The supernatants were transferred into a new 96-well plate and incubated with LDH working reagent for 30 min. The OD values were detected at 450 nm using a 680 iMark microplate reader (Bio-Rad, USA).

Calcein-AM Staining

MLO-Y4 cells were treated with NaF (0, 4, 8 mmol/L) for 24 h. Afterward, cells were washed twice in PBS and incubated with Calcein-AM (5 µmol/L) at 37 °C for 15 min in the dark. Cells were washed and visualized using a fluorescence microscope (Leica DM 3000, Wetzlar, Germany) at an excitation/emission wavelength of 488/517 nm.

Hoechst 33,342 Staining

MLO-Y4 cells were treated with NaF (0, 4, 8 mmol/L) for 24 h. Then, cells were washed twice in PBS, fixed with 4% paraformaldehyde for 10 min, and washed 3 times in PBS. Subsequently, the cells were stained with Hoechst 33,342 (5 µg/mL) at room temperature for 10 min in the dark. Cells were washed in PBS and visualized using a light microscope (Leica 300, Wetzlar, Germany) with an excitation/emission wavelength of 351/461 nm.

Cell Cycle Analysis

MLO-Y4 cells were treated with NaF (0, 4, 8 mmol/L) for 24 h, collected, and fixed in pre-cooled 75% ethanol. Then, cells were washed in PBS and stained with propidium iodide (PI, 50 µg/mL) for 5 min in the dark. The DNA content was detected by flow cytometry (BD Biosciences, Bedford, MA, USA) at 488 nm. The data were analyzed using CellQuest software (BD Biosciences, NJ, USA), and the percentage in the G0/G1 phase and the G2/M phase were calculated using the MODFIT software.

Detection of Cell Apoptosis

MLO-Y4 cells were treated with NaF (0, 4, 8 µmol/L) for 24 h. Cells were collected and stained with Annexin V/PI (5 µg/mL) for 15 min in the dark. Then, cells in each tube

were added 200 µL binding buffer and analyzed using a FACSCalibur (BD Biosciences, Bedford, MA, USA). At least 10,000 cells were analyzed in each sample, and the percentage of apoptosis was performed using CellQuest software (Becton–Dickinson, USA).

Measurement of Caspase-3 and Caspase-9 Activities

MLO-Y4 cells were treated with NaF (0, 4, 8 mmol/L) for 24 h and collected to detect the activity of caspase-3 and caspase-9 using the commercial kits, according to the manufacturer's instructions.

Detection of Autophagosome Flux

Autophagy flux was detected using a Cyto-ID autophagy detection kit according to the manufacturer's instructions. MLO-Y4 cells were treated with NaF (0, 4, 8 mmol/L) for 24 h. Then, the treated cells were collected and stained with the diluted Cyto-ID solution at 250 µL at room temperature for 30 min in the dark. The green fluorescent Cyto-ID intensity was analyzed using a FACSCalibur (BD Biosciences, Bedford, MA, USA) at 488 nm.

Lysosomes Detection with LysoTracker Red Staining

MLO-Y4 cells (1×10^4 cells/mL) were treated with NaF (0, 4, 8 mmol/L) for 24 h. The treated cells were incubated with LysoTracker Red, a lysosomotropic probe (50 nmol/L, Invitrogen), for 30 min at 37 °C and photographed using a fluorescence microscope (Leica DM3000, Wetzlar, Germany).

Detection of Intracellular Adenosine Triphosphate (ATP) Content

MLO-Y4 cells were treated with NaF (0, 4, 8 mmol/L) for 24 h, and the concentrations of intracellular ATP were measured using an ATP assay kit following the manufacturer's protocols.

Evaluation of Mitochondrial Membrane Potential (MMP)

The MMP level was measured with a JC-1, a lipophilic probe that potential-dependently accumulated in mitochondria, and its fluorescence emission shifted from red (590 nm, J-aggregates) to green (525 nm, J-monomers) when MMP was decreasing. In brief, MLO-Y4 cells were treated with NaF (0, 4, 8 mmol/L) for 24 h, rinsed twice in PBS, and then stained with JC-1 (1 µmol/L) for 20 min at 37 °C in the dark. The fluorescence images of J-monomers (red) and J-aggregates (green) were obtained using a Leica 300 fluorescent microscope (Wetzlar, Germany). In addition, the

NaF-treated MLO-Y4 cells were ingested and collected to quantitatively analyze the level of MMP using flow cytometry (BD Biosciences, NJ, USA). For statistical significance, at least 10,000 cells were analyzed in each sample.

Observation of Mitochondrial Structure

MLO-Y4 cells were treated with NaF (0, 4, 8 mmol/L) for 24 h. Afterward, cells were washed in PBS twice and incubated with MitoTracker Green (1 μ mol/L) for 15 min in the dark. The fluorescence images of mitochondria were obtained under a Leica 300 fluorescent microscope (Wetzlar, Germany).

Measurement of Intracellular ROS and mtROS

The level of intracellular and mtROS was examined by the uptake of dichlorodihydrofluorescein diacetate (DCFH-DA) Green and MitoSOX Red, according to our previous report [35, 37]. Briefly, MLO-Y4 cells were treated with NaF (0, 4, 8 mmol/L) for 6 h. Thereafter, cells were incubated with DCFH-DA (10 μ mol/L) and MitoSOX (5 μ mol/L), respectively, at 37 °C for 30 min in the dark, and washed twice in PBS. Images were acquired using a Leica DM 3000 fluorescent microscope (Leica, Wetzlar, Germany). To quantitate the levels of ROS and mtROS, the green and red fluorescences were detected by a FACSCalibur (Beckman Coulter, Brea, CA, USA).

Evaluation of Malondialdehyde (MDA) Content, Glutathione (GSH) Level, and Superoxide Dismutase (SOD) Activity

MLO-Y4 cells were treated with NaF (0, 4, 8 mmol/L) for 24 h. After removing the supernatants, MDA content, GSH level, and SOD activity were examined using commercial detection kits according to the manufacturer's instructions.

Preparation of Protein Extracts and Western Blot Analysis

MLO-Y4 cells were treated with NaF (0, 4, 8 mmol/L) for 24 h. The cells were collected and lysed in ice-cold RIPA buffer containing PMSF and phosphatase inhibitors. Then, the samples were separated by 12% SDS-PAGE and transferred electrophoretically onto a PVDF membrane. The membrane was blocked in TBST with 5% BSA for 2 h and incubated with the primary antibodies against cyclin D1, proliferating cell nuclear antigen (PCNA), cytochrome c (Cyto-c), Bcl-2, Bax, microtubule-associated protein light chain 3 (LC-3) II, p62, PTEN-induced putative kinase (PINK)1, Parkin, and β -actin at 4 °C overnight. After being washed in TBST, the membrane was incubated with HRP

conjugated goat anti-rabbit-IgG secondary antibody at 37 °C for 2 h. After washing in TBST again, the protein bands were detected using the ECL chemiluminescence detection system. Densitometric analysis was analyzed using Quality One 4.50 (Bio-Rad, USA).

Statistical Analysis

All statistical analyses were performed using the GraphPad Prism 7 (GraphPad Software, Inc., La Jolla, CA, USA). Quantitative data were expressed as means \pm SD and represented the results of at least three independent experiments. Statistical significance was determined using the unpaired Student's *t*-test between the two groups. For comparison among multiple groups, the one-way analysis of variance (ANOVA) was used. $P < 0.05$ was considered significant.

Results

NaF Exposure Caused Cell Death of Osteocytes MLO-Y4

To observe the cytotoxic effect of NaF exposure on MLO-Y4 cells, CCK-8, LDH release, and Calcein-AM staining were performed. As shown in Fig. 1, MLO-Y4 cells showed no obvious cytotoxicity when exposed to low doses of NaF (<2 mmol/L) for 24 h (Fig. 1A). However, when the concentrations of NaF increased to 2–10 mmol/L, NaF exposure caused a remarkable cytotoxic effect and elevated release of LDH (Fig. 1B), resulting in evident morphological alterations characterized by cellular shrinkage, reduction of cell volume, and density (Fig. 1C). Furthermore, the adverse effect was in a dose-dependent manner. In addition, we determined that the IC₅₀ value of NaF was almost 8 mmol/L for 24 h in MLO-Y4 cells. Therefore, we chose the test dose of NaF (4 mmol/L, 8 mmol/L) based on the IC₅₀ value in our following mechanism experiments.

NaF Exposure Promoted G2/M Phase Arrest and Apoptosis in MLO-Y4 Cells

To investigate whether NaF exposure affected the progression of the cell cycle, MLO-Y4 cells were treated with NaF (0, 4, 8 mmol/L) for 24 h, and cell cycle distribution was evaluated using flow cytometry to analyze cellular DNA content. As shown in Fig. 2A, NaF exposure remarkably blocked the cell cycle progression in the G2/M phase and increased the percentage of cells in the G2/M phase, with the proportion in G2/M phase cells rising from 10.48 (control) to 11.53% (0.5 mmol/L) or 21.57% (2 mmol/L) (Fig. 2A and B). Moreover, NaF exposure decreased the levels of cell

Fig. 1 NaF exposure caused cell death of MLO-Y4 cells. MLO-Y4 cells were treated with various concentrations of NaF (0, 0.25, 0.5, 1, 2, 4, 8, 10 mmol/L) for 24 h, and the cell viability was examined by **A** CCK-8, **B** LDH release assay, and **C** Calcein-AM staining. Quantitative data are presented as mean \pm SD of four independent experiments. The unpaired Student's *t*-test was conducted. * $P < 0.05$ and ** $P < 0.01$ compared with the control group

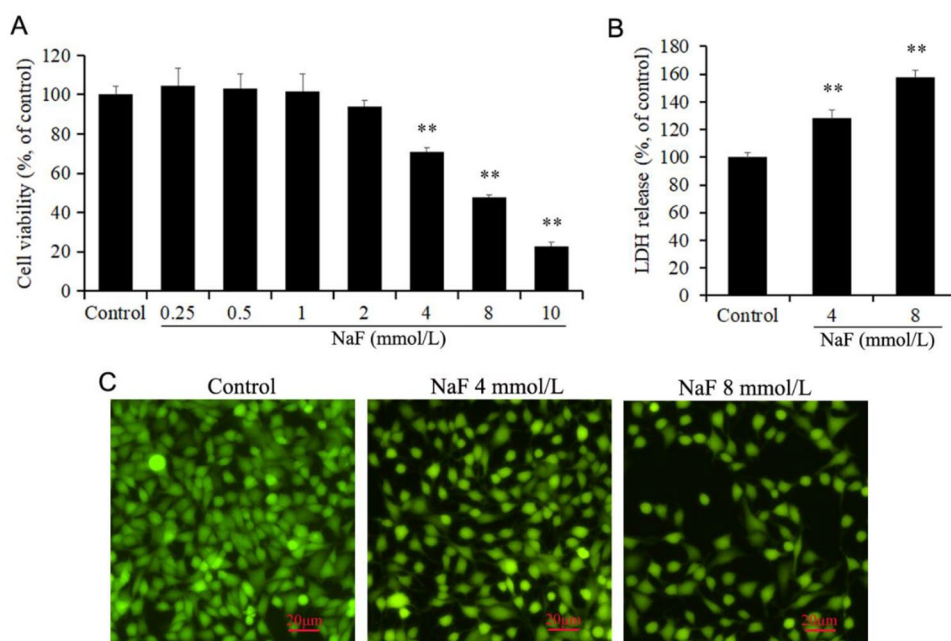
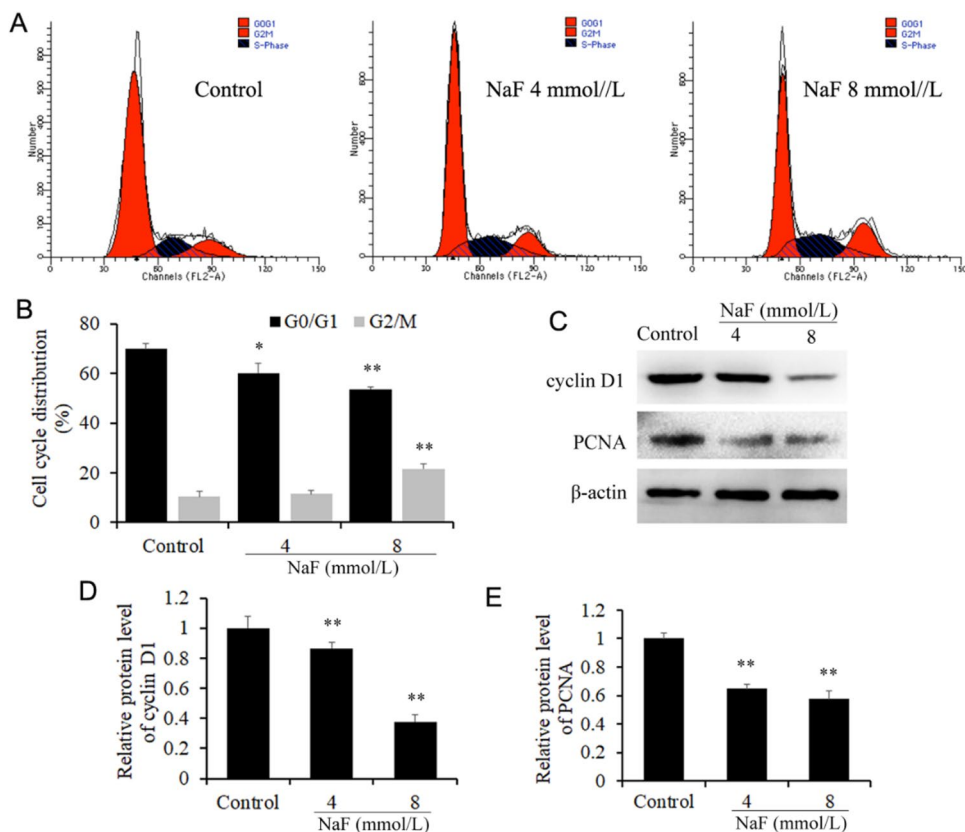


Fig. 2 NaF exposure promoted cell cycle G2/M arrest in MLO-Y4 cells. MLO-Y4 cells were treated with NaF (0, 4, 8 mmol/L) for 24 h, and **A** and **B** the distribution of the cell cycle was determined by flow cytometry; **C** protein levels of cyclin D1 and PCNA were examined using western blotting; **D** and **E** densitometric data were quantified using Quality One 4.50. Quantitative data are presented as mean \pm SD of four independent experiments. The unpaired Student's *t*-test was conducted. * $P < 0.05$ and ** $P < 0.01$ compared with the control group



cycle-associated proteins cyclin D1 and PCNA (Fig. 2C), and NaF (8 mmol/L) suppressed protein expressions of cyclin D1 and PCNA more obviously, and they were reduced to 37.72% and 57.48% of control, respectively (Fig. 2D and E). In addition, chromatin condensation assays with PI staining

demonstrated NaF-induced nuclear apoptosis. Untreated cells were uniformly stained with round nuclei, while the NaF-treated MLO-Y4 cells showed typical apoptotic changes such as nuclear enrichment, nuclear brightening, and fragmentation (Fig. 3A). Flow cytometric analysis further

revealed that NaF indeed increased apoptosis of MLO-Y4 cells (Fig. 3B and C), and the numbers of apoptosis were increased from 3.90 (control) to 10.63% (4 mmol/L) and 23.28% (8 mmol/L). Then, NaF exposure induces apoptotic cell death in MLO-Y4 cells.

NaF Exposure Caused Mitochondria Damage and Triggered Mitochondria-Dependent Apoptosis in MLO-Y4 Cells

Mitochondria play a vital major role in apoptosis triggered by many stimuli including fluoride [38]. To ascertain whether mitochondrial alterations occurred in the process of NaF-induced apoptotic cell death of MLO-Y4 cells, we examined the level of MMP and ATP production and

mitochondrial morphological alterations in MLO-Y4 cells. As shown in Fig. 4, NaF exposure dose-dependently caused loss of MMP, with an increase in green fluorescence and a decline in red fluorescence. In the NaF-treated groups, the green fluorescence intensities were increased to 78.82% (4 mmol/L) and 42.56% (8 mmol/L) of control, respectively (Fig. 4A and B). Moreover, NaF exposure reduced the production of intracellular ATP (Fig. 4D) in MLO-Y4 cells and disrupted the mitochondrial structure, converting the mitochondrial tubular shape to punctate dot-like fragments (Fig. 4B). Western blotting data showed that NaF treatment significantly upregulated Bax/Bcl-2 ratio and Cyto c release and increased the activities of caspase-3 and caspase-9 (Fig. 4E–I). These observations suggest that NaF exposure induces the release of cytochrome c from the mitochondria

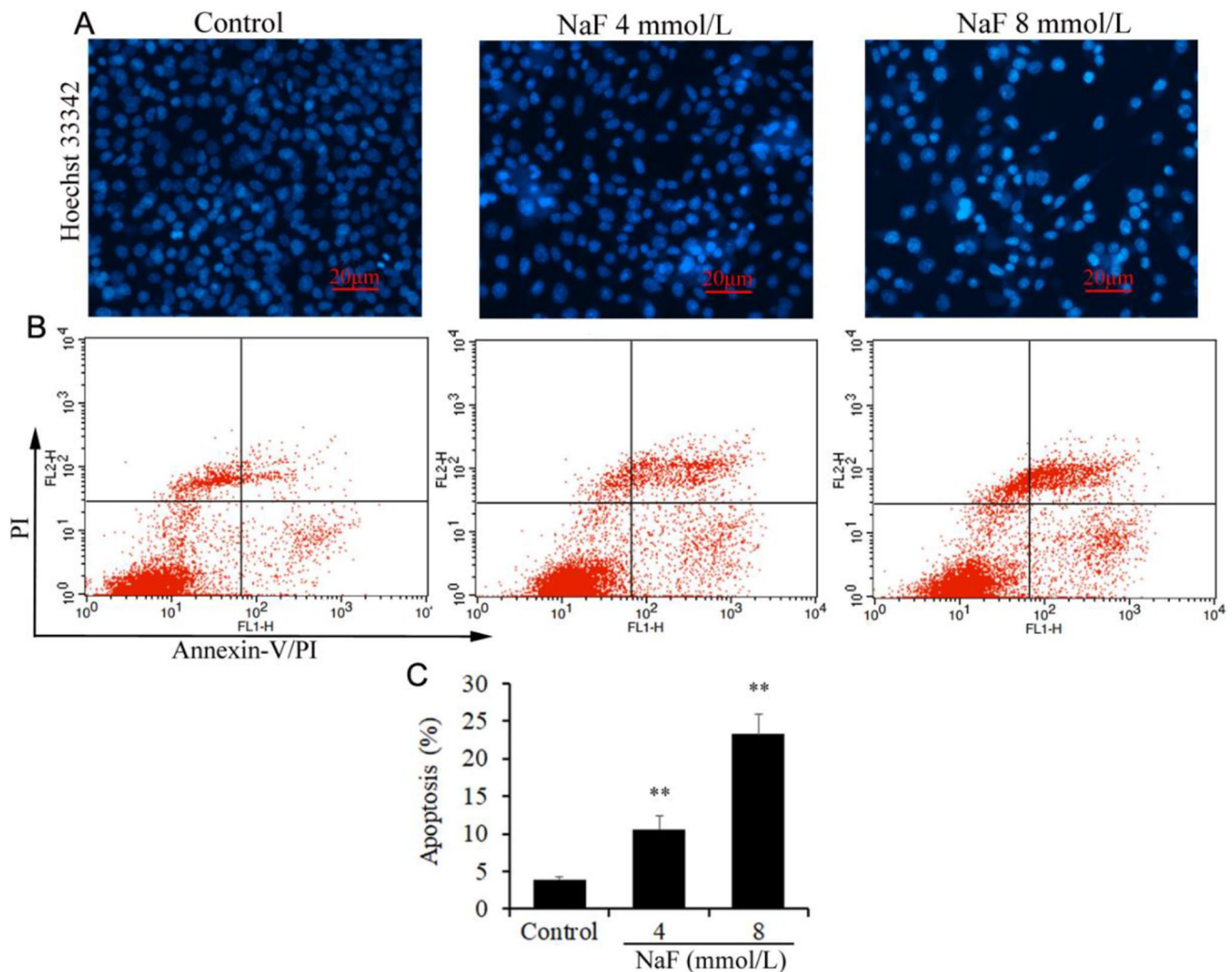


Fig. 3 NaF exposure increased cellular apoptosis in MLO-Y4 cells. MLO-Y4 cells were treated with NaF (0, 4, 8 mmol/L) for 24 h, **A** labeled with Hoechst 33,342, and observed using a Nikon 300 light microscope; **B** and **C** cells were stained with Annexin-V/PI double

staining and subjected to cytometric analysis for apoptosis. Quantitative data are presented as mean \pm SD of three independent experiments. The unpaired Student's *t*-test was conducted. ** $P < 0.01$ compared with the control group

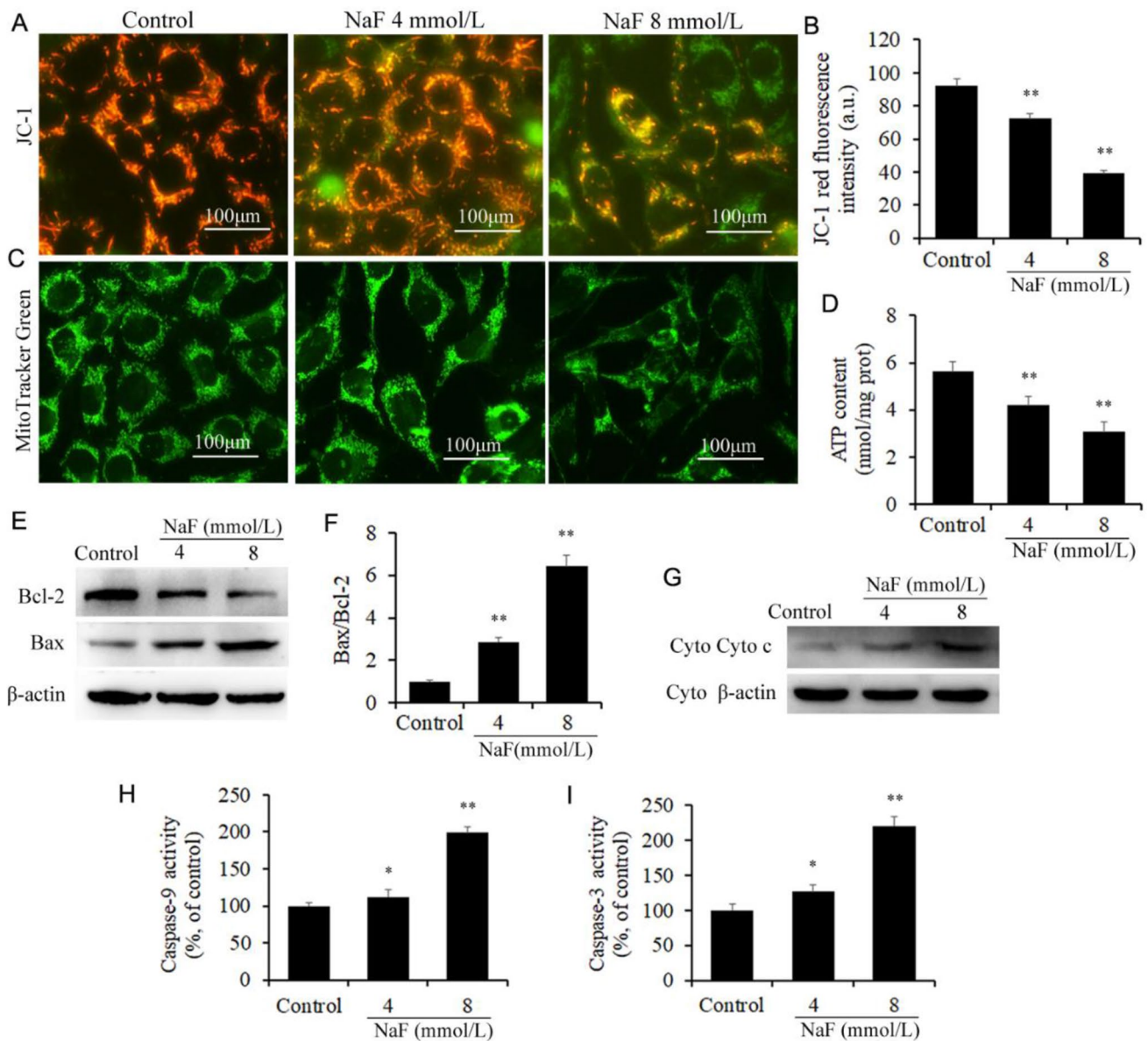


Fig. 4 NaF exposure caused mitochondrial damage and triggered mitochondrial-dependent apoptosis in MLO-Y4 cells. MLO-Y4 cells were treated with NaF (0, 4, 8 mmol/L) for 24 h, and **A** and **C** the level of MMP was detected by a Nikon 300 light microscope and flow cytometry using JC-1 staining; **B** mitochondrial morphological changes were observed by MitoTracker Green staining; **D** ATP content was examined by a luminometer; **E** and **G** protein expressions of

Bcl-2, Bax, and cytochrome C were examined by western blotting; **F** the ratio of Bax/Bcl-2 was quantified using Quality One 4.50. **H** and **I** the activities of caspase-3 and caspase-9 were examined by ELISA. Quantitative data are presented as mean \pm SD of four independent experiments. The unpaired Student's *t*-test was conducted. * $P < 0.05$ and ** $P < 0.01$ compared with the control group

to the cytosol and confirms the occurrence of mitochondria-dependent intrinsic apoptosis in MLO-Y4 cells.

NaF Exposure Increased Mitophagy in MLO-Y4 Cells

PINK1, Parkin, LC3, and p62 are central autophagy-related proteins involved in mitophagy [27–29, 32]. We identified that NaF exposure significantly induced activation of mitophagy and upregulated the expression of LC3-II,

PINK1, and Parkin (Fig. 5A–D), compared with control group; while the level of p62 was reduced in NaF-treated cells (Fig. 5A and E). To monitor autophagy flux and autophagic acidic compartments, the Cyto-ID autophagy detection kit and the LysoTracker Red probe were performed. The flow cytometric data indicated that NaF exposure increased autophagy flux, and the Cyto-ID green fluorescent intensities were increased from 19.05 (control) to 24.01% (4 mmol/L), to 34.39% (8 mmol/L) (Fig. 5F and G).

Fluorescent staining showed that NaF significantly accelerated the accumulation of acidic vacuoles and increased the percentages of cells with red-stained lysosomes (Fig. 5H), which was similar to those results of flow cytometric analysis and immunoblotting (Fig. 5A–G). These results suggest that NaF exposure caused cell damage or even death of MLO-Y4 cells, closely associated with increasing mitophagy.

NaF Exposure Promoted ROS Production and Induced Oxidative Stress in MLO-Y4 Cells

ROS are produced in mitochondria, and excessive ROS generated leads to apoptosis and mitophagy [26]. To better understand the role of ROS in regulating NaF-induced apoptosis and mitophagy in MLO-Y4 cells, we examined the levels of intracellular ROS and mtROS after NaF treatment for 6 h. Fluorescence data and flow cytometric analysis demonstrated that NaF exposure dose-dependently triggered the production of intracellular ROS and mtROS (Fig. 6A–D). Moreover, NaF treatment significantly increased MDA content (Fig. 6E), while it reduced SOD activity and GSH level (Fig. 6F and G). Thus, NaF exposure triggers ROS generation and induces oxidative stress, which may increase cell apoptosis and mitophagy in MLO-Y4 cells.

ROS Contributed to Cell Apoptosis and Mitophagy Caused by NaF in MLO-Y4 Cells

As expected, the ROS scavenger N-acetylcysteine (NAC) remarkably reversed mitochondrial damage and cell apoptosis caused by NaF exposure (Fig. 7A and B). Moreover, NAC significantly inhibited NaF-induced mitophagy, shown by lower expressions of LC-3II, PINK1, and Parkin (Fig. 7C–F), and obvious reductions in autophagy flux and the accumulation of acidic vacuoles (Fig. 7G and H). These data strongly confirm that the excess ROS induced by NaF exposure can trigger cell apoptosis and mitophagy in MLO-Y4 cells.

Discussion

Fluorine, an active element, is essential for the proper development of bones and teeth [1, 8, 9]. Nevertheless, excessive fluoride intake may disturb bone turnover, which causes skeletal and dental fluorosis as it induces aberrant activation of osteoblasts in the early stage [10–12]. Furthermore,

higher levels of fluoride cause cellular apoptosis of osteoblasts and promote osteoclastic bone loss [13–15]; this ultimately results in abnormality metabolism of bone in mice with skeletal fluorosis. In comparison to studies on the relationship between fluoride and osteoblasts and osteoclasts, little data is available on how it affects osteocytes comprising more than 95% of the bone cells [17, 18]. Here, we reported that NaF exposure increased the generation of intracellular ROS and mtROS, provoked mitochondria-mediated apoptosis, and increased mitophagy in MLO-Y4 cells; pretreatment with the ROS scavenger NAC significantly prevented NaF-induced apoptosis and mitophagy. Our results first reveal that ROS-mediated apoptosis and mitophagy are the cellular mechanisms for the toxic effect of NaF on osteocytes, thereby helping our understanding of the potential role of osteocytes in skeletal and dental fluorosis.

In the present study, we first demonstrated that NaF (4, 8 mmol/L) treatment for 24 h dose-dependently decreased cell viability and elevated LDH level and morphological alterations, implying that NaF exposure can cause cell membrane damage, increase LDH release, and eventually lead to cell death in MLO-Y4 cells. The cytotoxic effects were similar to the effect of NaF on osteoblast and osteoclast precursor RAW 264.7 macrophages [13–15], whereas the minimum concentrations of NaF required for inducing cell death of MLO-Y4 cells were higher than that of NaF on the above cells [13–15]. These investigations suggest that osteocytes may be less sensitive to cytotoxicity induced by NaF than osteoblasts and osteoclast precursors [13–15]. Moreover, NaF exposure induced G0/G1 phase arrest and increased the percentage of apoptosis in MLO-Y4 cells, which can release multiple osteoclastogenic factors including TNF- α and IL-6 to recruit osteoclasts and accelerate bone loss [23, 39]. These pro-apoptotic effects were consistent with a previous finding observed in another osteocyte-like line, IDG-SW3 after NaF treatment [24]. But the experimental concentrations of fluoride-induced apoptosis of MLO-Y4 cells were much higher than those of fluoride (16 mg/L, approximately 0.4 mmol/L) on IDG-SW3 cells [24]; what causes these differences still needs further investigation in the future. Based on this information, we speculate that NaF exposure can cause cell apoptosis of MLO-Y4 cells. However, the exact death mechanisms are still not investigated.

It is well known that the intrinsic apoptosis pathways are mitochondria-initiated events and involve a diverse array of non-receptor-mediated stimuli including fluoride, free radicals, and hypoxia [25, 38, 40]. These stimuli target the inner mitochondrial membrane and lead to the opening of the mitochondrial permeability transition pores, loss of the MMP, ATP synthesis reduction, and the translocation of Bax into mitochondria, thereby causing the release of Cyt c from the mitochondria into the cytosol [25, 41, 42]. Once released into the cytoplasm, Cyt c can bind other

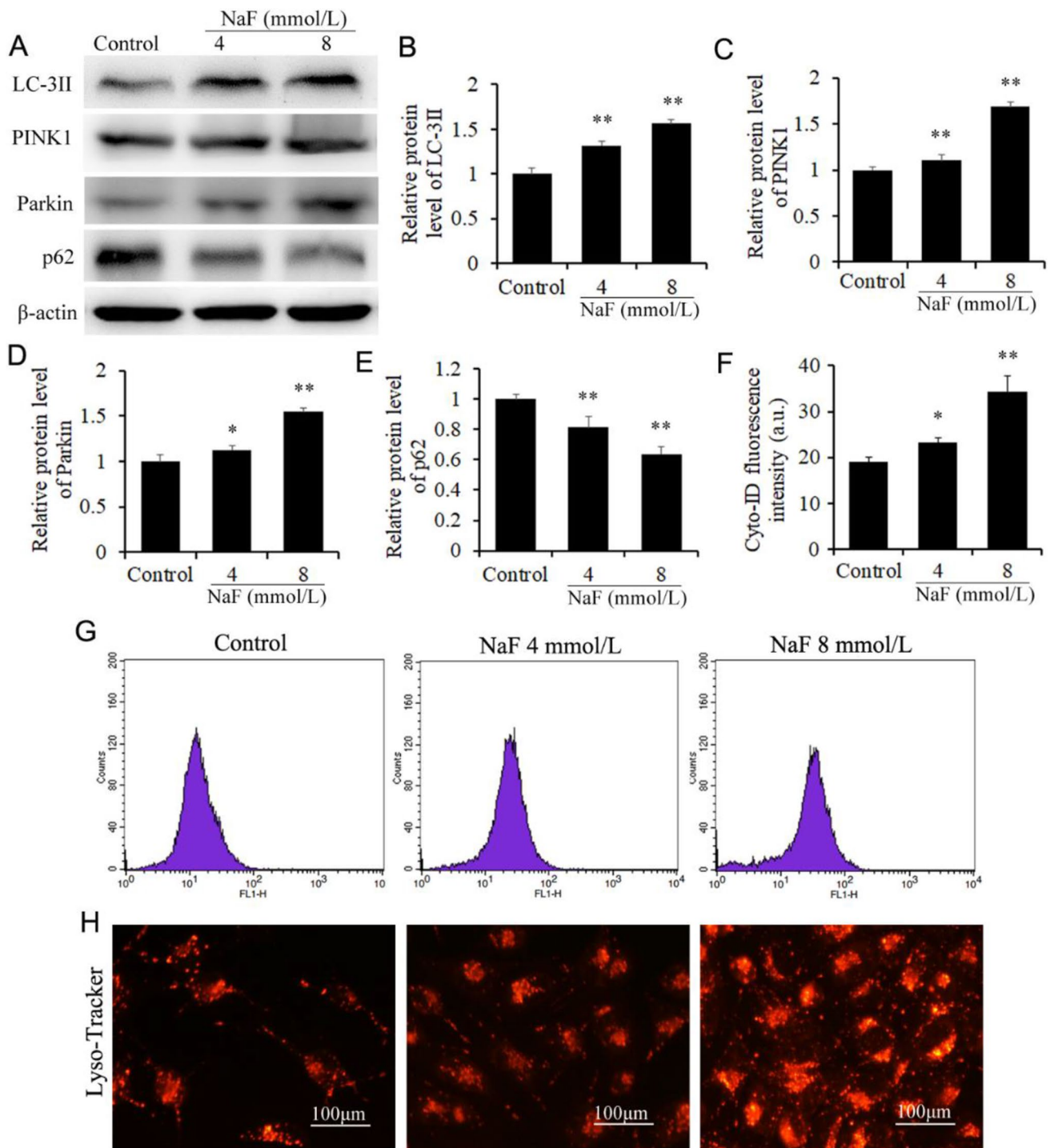


Fig. 5 NaF exposure induced mitophagy in MLO-Y4 cells. MLO-Y4 cells were treated with NaF (0, 4, 8 mmol/L) for 24 h. **A** Protein expressions of LC-3II, p62, PINK1, and Parkin were examined by western blotting; **B**, **C**, **D**, and **E** densitometric data were quantified using Quality One 4.50; **G** autophagy flux was detected by flow cytometry using the Cyto-ID autophagy detection kit, and **F** Cyto-

ID fluorescence intensity was represented; **H** the accumulation of acidic vesicles was observed using LysoTracker Red staining. Quantitative data are presented as mean \pm SD of five independent experiments. The unpaired Student's *t*-test was conducted. * $P < 0.05$ and ** $P < 0.01$ compared with the control group

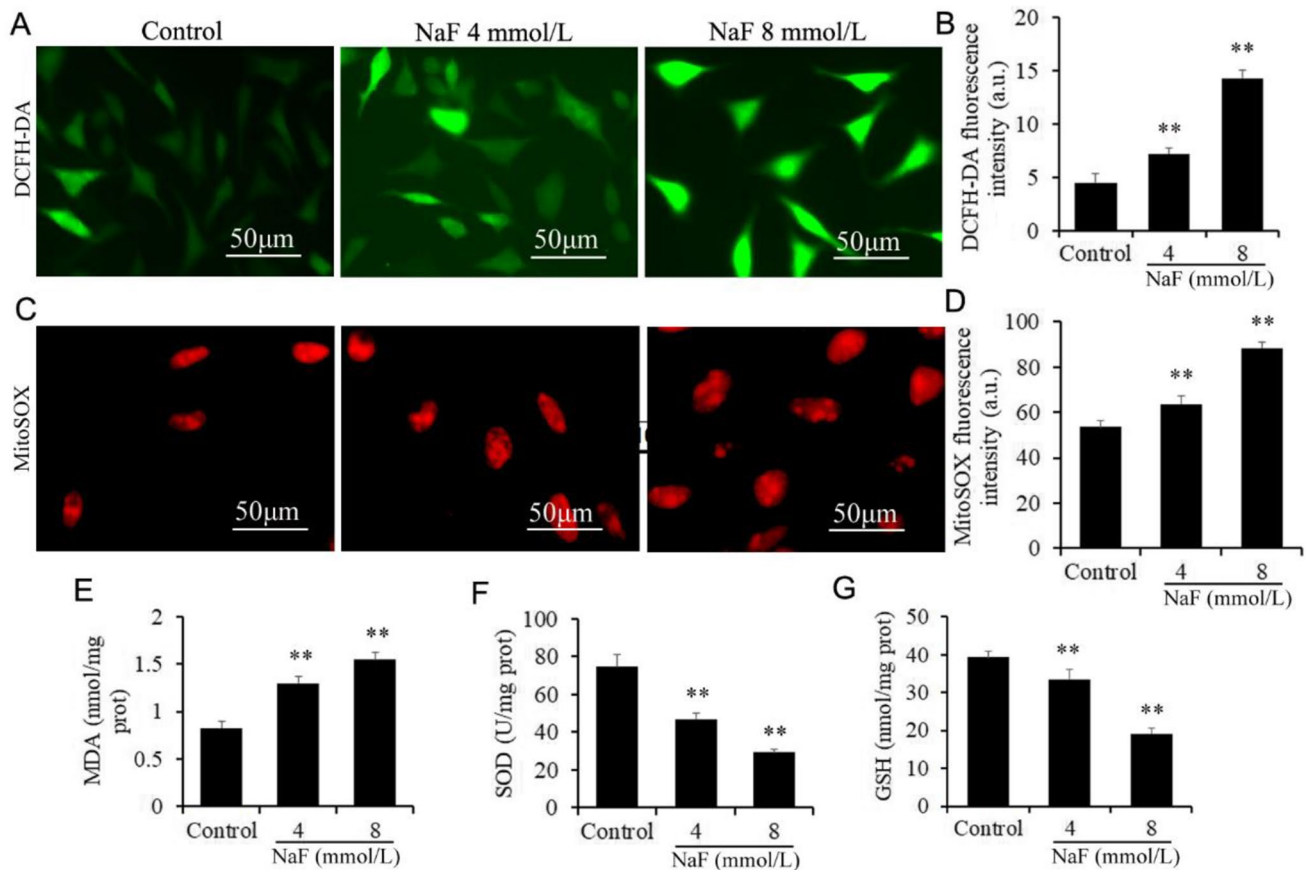


Fig. 6 NaF exposure promoted ROS generation and caused oxidative stress in MLO-Y4 cells. MLO-Y4 cells were treated with NaF (0, 4, 8 mmol/L) for 6 h, and **A** and **B** the levels of intracellular ROS were examined by DCFH-DA fluorescence staining using a Nikon 300 light microscope and flow cytometry; **C** and **D** the levels of mtROS were examined by MitoSOX fluorescence staining using a Nikon 300

light microscope and flow cytometry; **E**, **F**, and **G** the MDA content, SOD activity, and GSH level were determined by chemical colorimetry. Quantitative data are presented as mean \pm SD of three independent experiments. The unpaired Student's *t*-test was conducted. ***P* < 0.01 compared with the control group

molecules, form an apoptotic body to activate caspase-3 and caspase-9, and trigger apoptosis [42]. Most studies have revealed that either directly or indirectly fluoride exposure damages mitochondrial membrane integrity [43], reduces the overall activity of the mitochondria, inhibits cellular respiration, and triggers leakage of free radicals and cytochrome c, ultimately inducing oxidative damage [44]. In addition, fluoride reduces intracellular ATP synthesis and triggers the c-Jun N-terminal kinase (JNK)-mediated apoptosis, which may lead to impairment of ameloblast function and dental fluorosis [45]. In the present study, we found that NaF exposure also caused mitochondrial damage, as observed by loss of MMP, intracellular ATP reduction, and a large number of mitochondrial fragments. Moreover, exposure to NaF upregulated the Bax/Bcl-2 ratio and promoted Cyt c released, which increased the enzymatic activity of caspase-9 and caspase-3, thereby initiating the mitochondria-mediated apoptosis pathway [25, 38–42]. Taken together, this evidence

demonstrates that NaF exposure promotes cell apoptosis through the mitochondria-mediated signaling pathway.

Recently, several studies have demonstrated that mitophagy is responsible for the toxicity of environmental pollutants to skeletal health, especially on bone cells [26–29]. Mitophagy can regulate the proliferation, differentiation, and function of osteoblasts under type 2 diabetes, hypoxia, and aluminum-overload stress [26, 32, 33]; Increasing mitophagy level leads to low bone mass, osteoporosis, and apical periodontitis [32, 33]. Moreover, a previous in vitro study reported that mitophagy in osteocytes was remarkably increased by hypoxia, which led to osteoclastogenesis and bone loss in dexamethasone-induced osteonecrosis of the femoral head [34]. In agreement with these results, NaF exposure also increased the levels of mitophagy-associated proteins like LC3II, PINK1, and Parkin, together with a declined expression of p62, which interacts with LC3II, and is degraded in autophagolysosomes [26, 27]. Furthermore,

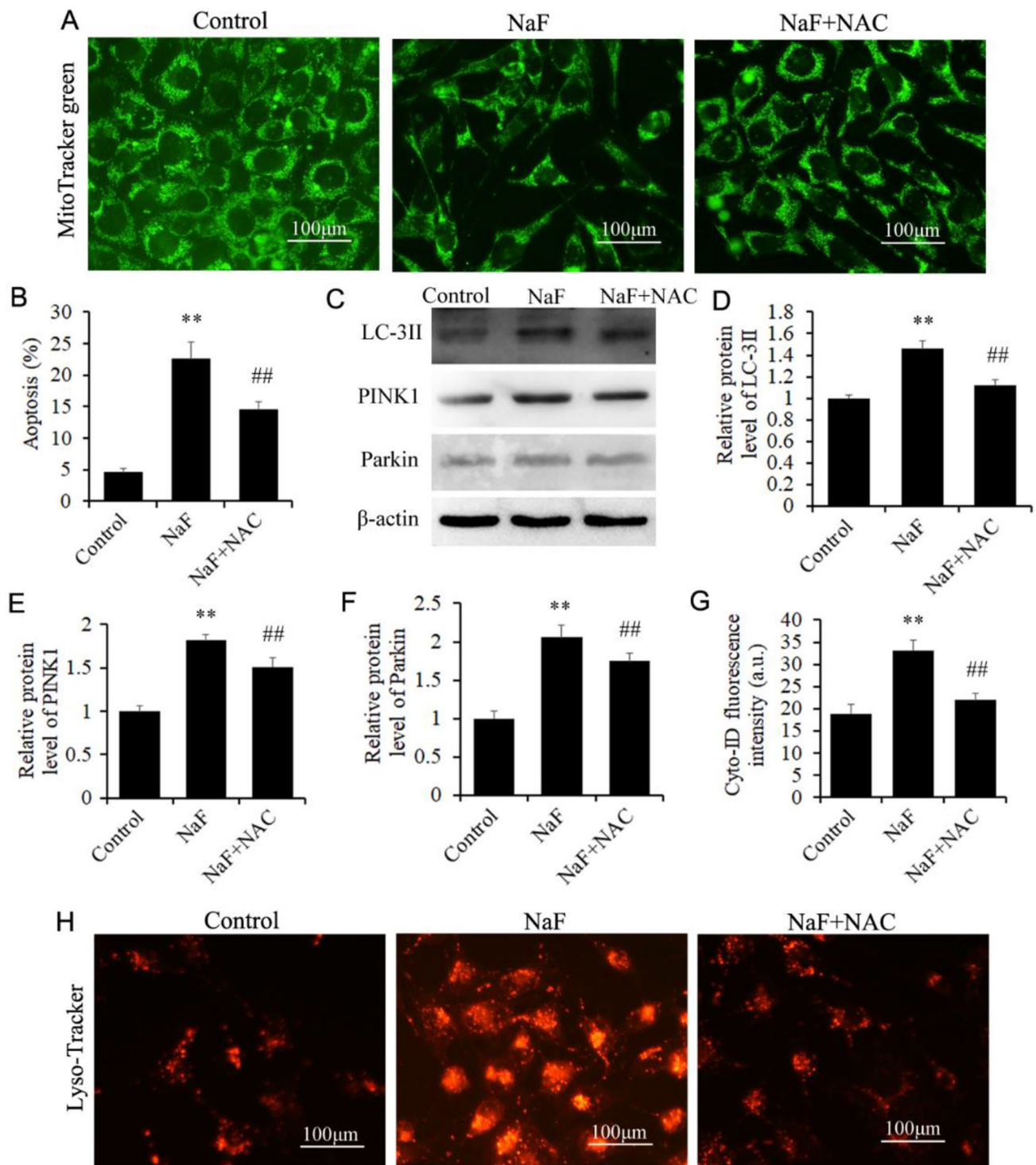


Fig. 7 Effect of NAC on NaF-induced apoptosis and mitophagy in MLO-Y4 cells. MLO-Y4 cells were pretreated with NAC (2 mmol/L) for 2 h and then incubated with NaF (0, 4, 8 mmol/L) for 24 h. **A** Mitochondrial morphological changes were observed by MitoTracker Green staining. **B** Cell apoptosis was determined by Annexin-V/PI double staining using flow cytometry; **C** the protein expressions of LC-3II, PINK1, and Parkin were detected by western blotting; **D**, **E**, and **F** densitometric analysis was analyzed by Quality One 4.50;

G autophagy flux was detected by flow cytometry using the Cyto-ID autophagy detection kit; **H** the accumulation of acidic vesicles was observed using LysoTracker Red staining. Quantitative data are presented as mean \pm SD of three independent experiments. The unpaired Student's *t*-test or one-way ANOVA was conducted. ** $P < 0.01$ compared with the control group; ## $P < 0.01$ compared with NaF (8 mmol/L)-treated group

NaF promoted the elevation of the autophagy flux and the accumulation of acidic vacuole, implying that autophagosomes fuse with lysosomes to form autolysosomes. These results indicate that excessive fluoride induces autophagy in the form of mitophagy. The acidic vacuole releases its contents through autophagic flux into the microenvironment of osteocytes, and it may induce matrix proteolysis and demineralization of bone around osteocytes that over time may lead to localized bone destruction. Hence, we speculate that, in addition to apoptosis, mitophagy may be another novel pathway mediating fluoride-induced cell death of osteocytes.

ROS have been considered to be a driving force for apoptosis and mitophagy as they induce the permeability of the mitochondrial membrane, damage the respiratory chain, and ultimately trigger the apoptotic and mitophagic signal pathways [25–27, 44]. Current literature described that the induction of massive ROS directly related to the mitochondria-dependent apoptosis and activation of the PINK1/Parkin pathway, which exerted obvious toxicity to osteoblasts and led to abnormal bone metabolism [46, 47]. Meanwhile, Li et al. reported that fluoride exposure triggered the generation of ROS and increased oxidative stress, associated with fluoride toxicity on bone [48]. Similar to these observations, this study showed that NaF exposure increased the production and accumulation of intracellular ROS and mtROS and elevated the levels of MDA together with the reductions in SOD activity and GSH content, which promotes oxidative stress response. This oxidative damage, in turn, can stimulate the production of ROS and mtROS [36, 45] and then accelerate cell death of MLO-Y4 cells. More importantly, inhibition of ROS generation with the ROS scavenger NAC remarkably decreased the number of apoptosis and mitochondria damage caused by fluoride exposure, suggesting that NAC is protected against fluoride-induced mitochondria-mediated apoptosis. With further investigation, we found that NAC pretreatment has also been shown to attenuate fluoride-induced mitophagy response, shown by lower expressions of LC-3II, PINK1, and Parkin and the recovery of mitochondrial function. Thus, NaF can induce the generation of ROS, which triggers the mitochondria-mediated apoptosis mitophagy caused by fluoride exposure in MLO-Y4 cells.

Conclusion

The present study suggests that NaF directly promoted the production of intracellular ROS and mtROS, triggered G2/M phase arrest, and ultimately led to mitochondria-mediated apoptosis and mitophagy in MLO-Y4 cells. These cytotoxic effects were reversed by the ROS scavenger NAC, implying

that NaF exposure induces apoptosis and mitophagy via increasing ROS production. This study first provides in vitro evidence that apoptosis and mitophagy are cellular mechanisms for the toxic effect of NaF on osteocytes, thereby advancing our understanding of the potential role of osteocytes in skeletal and dental fluorosis.

Author Contribution Yun Zhang conceived and designed the experiments. Fanhe Dong, Zihan Wang, Bingbing Xu, and Qiqi Wang carried out the experiments. Tao Zhang and Qiao Lin processed the data. Yun Zhang and Fanhe Dong wrote the paper. The final manuscript was read and approved by all authors.

Funding This work was supported by the Natural Science Foundation of Zhejiang Province (LY21H060001), the National Natural Science Foundation of China (30900301), and the National Undergraduate Innovation and Entrepreneurship Training Program (202110349006).

Data Availability The data of this study will be made available on reasonable request.

Declarations

Competing interests The authors declare no competing interests.

Conflict of Interest The authors declare no competing interests.

References

1. Jha SK, Mishra VK, Sharma DK, Damodaran T (2011) Fluoride in the environment and its metabolism in humans. *Rev Environ Contam Toxicol* 211:121–142. https://doi.org/10.1007/978-1-4419-8011-3_4
2. Abduweli UD, Goin DE, Martinez-Mier EA, Woodruff T, DenBesten P (2020) Maternal and fetal exposures to fluoride during mid-gestation among pregnant women in northern California. *Environ Health-Glob* 19:38. <https://doi.org/10.1186/s12940-020-00581-2>
3. Atmaca N, Atmaca HT, Kanici A, Anteplioglu T (2014) Protective effect of resveratrol on sodium fluoride-induced oxidative stress, hepatotoxicity and neurotoxicity in rats. *Food Chem Toxicol* 70:191–197. <https://doi.org/10.1016/j.fct.2014.05.011>
4. Wu L, Fan C, Zhang Z, Zhang X, Lou Q, Guo N, Huang W, Zhang M, Yin F, Guan Z, Yang Y, Gao Y (2021) Association between fluoride exposure and kidney function in adults: a cross-sectional study based on endemic fluorosis area in China. *Ecotoxicol Environ Saf* 225:112735. <https://doi.org/10.1016/j.ecoenv-2021-112735>
5. Quadri JA, Sarwar S, Pinky Kar P, Singh S, Mallick SR, Arava S, Nag TC, Roy TS, Shariff A (2018) Fluoride induced tissue hypercalcemia, IL-17 mediated inflammation and apoptosis lead to cardiomyopathy: ultrastructural and biochemical findings. *Toxicology* 406–407:44–57. <https://doi.org/10.1016/j-tox-2018-05-012>
6. Yuan J, Li Q, Niu R, Wang J (2019) Fluoride exposure decreased learning ability and the expressions of the insulin receptor in male mouse hippocampus and olfactory bulb. *Chemosphere* 224:71–76. <https://doi.org/10.1016/j.chemosphere-2019-02-113>
7. Zhang J, Li Z, Qie M, Zheng R, Shetty J, Wang J (2016) Sodium fluoride and sulfur dioxide affected male reproduction

- by disturbing blood-testis barrier in mice. *Food Chem Toxicol* 94:103–111. <https://doi.org/10.1016/j.fct.2016.05.017>
8. Dhar V, Bhatnagar M (2009) Physiology and toxicity of fluoride. *Indian J Dent Res* 20(3):350–355. <https://doi.org/10.4103/0970-9290-57379>
 9. Everett ET (2011) Fluoride's effects on the formation of teeth and bones, and the influence of genetics. *J Dent Res* 90:552–560. <https://doi.org/10.1177/00220-34510-384626>
 10. Qiao L, Liu X, He Y, Zhang J, Huang H, Bian W, Chilufya MM, Zhao Y, Han J (2021) Progress of signaling pathways, stress pathways and epigenetics in the pathogenesis of skeletal fluorosis. *Int J Mol Sci* 22(21):11932. <https://doi.org/10.3390/ijms222111932>
 11. Chu Y, Gao Y, Yang Y, Liu Y, Guo N, Wang L, Huang W, Wu L, Sun D, Gu W (2020) β -catenin mediates fluoride-induced aberrant osteoblasts activity and osteogenesis. *Environ Pollut* 265(Pt A):114734. <https://doi.org/10.1016/j.envpol-2020-114734>
 12. Xu H, Zhou YL, Zhang XY, Lu P, Li GS (2010) Activation of PERK signaling through fluoride-mediated endoplasmic reticulum stress in OS732 cells. *Toxicology* 277(1–3):1–5. <https://doi.org/10.1016/j.tox-2010-08-006>
 13. Gu X, Han D, Chen W, Zhang L, Lin Q, Gao J, Fanning S, Han B (2016) SIRT1-mediated FoxOs pathways protect against apoptosis by promoting autophagy in osteoblast-like MC3T3-E1 cells exposed to sodium fluoride. *Oncotarget* 7(40):65218–65230. <https://doi.org/10.18632/oncotarget-11573>
 14. Wang J, Zhao Y, Cheng X, Li Y, Xu H, Manthari RK, Wang J (2018) Effects of different Ca²⁺ level on fluoride-induced apoptosis pathway of endoplasmic reticulum in the rabbit osteoblast in vitro. *Food Chem Toxicol* 116(Pt B):189–195. <https://doi.org/10.1016/j.fct-2018-04-013>
 15. Yu H, Jiang N, Yu X, Zhao Z, Zhang X, Xu H (2018) The role of TGF β receptor 1-smad3 signaling in regulating the osteoclastic mode affected by fluoride. *Toxicology* 393:73–82. <https://doi.org/10.1016/j.tox-2017-11-009>
 16. Lv YG, Kang L, Wu G (2016) Fluorosis increases the risk of postmenopausal osteoporosis by stimulating interferon γ . *Biochem Biophys Res Commun* 479(2):372–379. <https://doi.org/10.1016/j.bbrc-2016-09-083>
 17. Bonewald LF (2017) The role of the osteocyte in bone and non-bone disease. *Endocrinol Metab Clin North Am* 46(1):1–18. <https://doi.org/10.1016/j.ecl-2016-09-003>
 18. Komori T (2013) Functions of the osteocyte network in the regulation of bone mass. *Cell Tissue Res* 352(2):191–198. <https://doi.org/10.1007/s00441-012-1546-x>
 19. Ru JY, Wang YF (2020) Osteocyte apoptosis: the roles and key molecular mechanisms in resorption-related bone diseases. *Cell Death Dis* 11:846. <https://doi.org/10.1038/s41419-020-03059-8>
 20. Huber C, Collishaw S, Mosley JR, Reeve J, Noble BS (2007) Selective estrogen receptor modulator inhibits osteocyte apoptosis during abrupt estrogen withdrawal: implications for bone quality maintenance. *Calcif Tissue Int* 81:139–144. <https://doi.org/10.1007/s00223-007-9049-6>
 21. Storlino G, Colaianni G, Sanesi L, Lippo L, Brunetti G, Errede M, Colucci S, Passeri G, Grano M (2020) Irisin prevents disuse-induced osteocyte apoptosis. *J Bone Miner Res* 35:766–775. <https://doi.org/10.1002/jbmr-3944>
 22. Farr JN, Xu M, Weivoda MM, Monroe DG, Fraser DG, Onken JL, Negley BA, Sfeir JG, Ogrodnik MB, Hachfeld CM, LeBrasseur NK, Drake MT, Pignolo RJ, Pirtskhalava T, Tchkonja T, Oursler MJ, Kirkland JL, Khosla S (2017) Targeting cellular senescence prevents age-related bone loss in mice. *Nat Med* 23(9):1072–1079. <https://doi.org/10.1038/nm.4385>
 23. Zhang Y, Yan M, Niu W, Mao H, Yang P, Xu B, Sun Y (2022) Tricalcium phosphate particles promote pyroptotic death of calvaria osteocytes through the ROS/NLRP3/Caspase-1 signaling axis in amouse osteolysis model. *Int Immunopharmacol* 107:108699. <https://doi.org/10.1016/j.intimp.2022.108699>
 24. Jiang N, Guo F, Xu W, Zhang Z, Jin H, Shi L, Zhang X, Gao J, Xu H (2020) Effect of fluoride on osteocyte-driven osteoclastic differentiation. *Toxicology* 436:152429. <https://doi.org/10.1016/j.tox-2020-152429>
 25. Yang J, Zhu Y, Zhang D, Yan Z, Zhao Y, Manthari RK, Cheng X, Wang J, Wang J (2021) Effects of different doses of calcium on the mitochondrial apoptotic pathway and Rho/ROCK signaling pathway in the bone of fluorosis rats. *Biol Trace Elem Res* 199(5):1919–1928. <https://doi.org/10.1007/s12011-020-02305-6>
 26. Cui Y, Song M, Xiao B, Liu M, Liu P, Han Y, Shao B, Li Y (2021) ROS-mediated mitophagy and apoptosis are involved in aluminum-induced femoral impairment in mice. *Chem Biol Interact* 349:109663. <https://doi.org/10.1016/j.cbi.2021.109663>
 27. Yin F, Yan J, Zhao Y, Guo KJ, Zhang ZL, Li AP, Meng CY, Guo L (2019) Bone marrow mesenchymal stem cells repair Cr (VI)-injured kidney by regulating mitochondria-mediated apoptosis and mitophagy mediated via the MAPK signaling pathway. *Ecotoxicol Environ Saf* 176:234–241. <https://doi.org/10.1016/j.ecoenv.2019.03.093>
 28. Avila-Rojas SH, Aparicio-Trejo OE, Sanchez-Guerra MA, Barbier OC (2022) Effects of fluoride exposure on mitochondrial function: energy metabolism, dynamics, biogenesis and mitophagy. *Environ Toxicol Pharmacol* 94:103916. <https://doi.org/10.1016/j.etap.2022.103916>
 29. Shen Y, Wu L, Qin D, Xia Y, Zhou Z, Zhang X, Wu X (2018) Carbon black suppresses the osteogenesis of mesenchymal stem cells: the role of mitochondria. *Part Fibre Toxicol* 15(1):16. <https://doi.org/10.1186/s12989-018-0253-5>
 30. Matsuda N, Sato S, Shiba K, Okatsu K, Saisho K, Gautier CA, Sou YS, Saiki S, Kawajiri S, Sato F, Kimura M, Komatsu M, Hattori N, Tanaka K (2010) PINK1 stabilized by mitochondrial depolarization recruits Parkin to damaged mitochondria and activates latent Parkin for mitophagy. *J Cell Biol* 189(2):211–221. <https://doi.org/10.1083/jcb-200910140>
 31. Ivankovic D, Chau KY, Schapira AH, Gegg ME (2016) Mitochondrial and lysosomal biogenesis are activated following PINK1/parkin-mediated mitophagy. *J Neurochem* 136(2):388–402. <https://doi.org/10.1111/jnc-13412>
 32. Wang X, Ma H, Sun J, Zheng T, Zhao P, Li H, Yang M (2022) Mitochondrial ferritin deficiency promotes osteoblastic ferroptosis via mitophagy in type 2 diabetic osteoporosis. *Biol Trace Elem Res* 200(1):298–307. <https://doi.org/10.1007/s12011-021-02627-z>
 33. Yang CN, Kok SH, Wang HW, Chang JZ, Lai EH, Shun CT, Yang H, Chen MH, Hong CY, Lin SK (2019) Simvastatin alleviates bone resorption in apical periodontitis possibly by inhibition of mitophagy-related osteoblast apoptosis. *Int Endod J* 52(5):676–688. <https://doi.org/10.1111/iej-13055>
 34. Xu K, Lu C, Ren X, Wang J, Xu P, Zhang Y (2021) Overexpression of HIF-1 α enhances the protective effect of mitophagy on steroid-induced osteocytes apoptosis. *Environ Toxicol* 36(11):2123–2137. <https://doi.org/10.1002/tox-23327>
 35. Zhang Y, Yan M, Shan W, Zhang T, Shen Y, Zhu R, Fang J, Mao H (2022) Bisphenol A induces pyroptotic cell death via ROS/NLRP3/Caspase-1 pathway in osteocytes MLO-Y4. *Food Chem Toxicol*. <https://doi.org/10.1016/j.fct-2021-112772>
 36. Bratic I, Trifunovic A (2010) Mitochondrial energy metabolism and ageing. *Biochim Biophys Acta* 1797(6–7):961–967. <https://doi.org/10.1016/j.bbabbio.2010.01.004>
 37. Zhang T, Shen Y, Zhu R, Shan W, Li Y, Yan M, Zhang Y (2022) Benzo[a]pyrene exposure promotes RIP1-mediated necroptotic death of osteocytes and the JNK/IL-18 pathway activation via generation of reactive oxygen species. *Toxicology* 476:153244. <https://doi.org/10.1016/j.tox-2022-153244>

38. Yan X, Wang L, Yang X, Qiu Y, Tian X, Lv Y, Tian F, Song G, Wang T (2017) Fluoride induces apoptosis in H9c2 cardiomyocytes via the mitochondrial pathway. *Chemosphere* 182:159–165. <https://doi.org/10.1016/j.chemosphere-2017-05-002>
39. Lv S, Zhang Y, Yan M, Mao H, Pan C, Gan M, Fan J, Wang G (2016) Inhibition of osteolysis after local administration of osthole in a TCP particles-induced osteolysis model. *Int Orthop* 40(7):1545–1552. <https://doi.org/10.1007/s00264-015-3021-2>
40. Yin J, Ni B, Liao WG, Gao YQ (2018) Hypoxia-induced apoptosis of mouse spermatocytes is mediated by HIF-1 α through a death receptor pathway and a mitochondrial pathway. *J Cell Physiol* 233(2):1146–1155. <https://doi.org/10.1002/jcp.25974>
41. Wang X, Ni H, Xu W, Wu B, Xie T, Zhang C, Cheng J, Li Z, Tao L, Zhang Y (2021) Difenoconazole induces oxidative DNA damage and mitochondria mediated apoptosis in SH-SY5Y cells. *Chemosphere* 283:131160. <https://doi.org/10.1016/j.chemosphere-2021-131160>
42. Li Z, Guo D, Yin X, Ding S, Shen M, Zhang R, Wang Y, Xu R (2020) Zinc oxide nanoparticles induce human multiple myeloma cell death via reactive oxygen species and Cyt-C/Apaf-1/caspase-9/caspase-3 signaling pathway in vitro. *Biomed Pharmacother* 122:109712. <https://doi.org/10.1016/j.biopha-2019-109712>
43. Zhao Y, Wang J, Zhang J, Sun Z, Niu R, Manthari RK, Ommati MM, Wang S, Wang J (2022) Fluoride exposure induces mitochondrial damage and mitophagy via activation of the IL-17A pathway in hepatocytes. *Sci Total Environ* 804:150184. <https://doi.org/10.1016/j.scitotenv.2021.150184>
44. Fina BL, Lombarte M, Rigalli JP, Rigalli A (2014) Fluoride increases superoxide production and impairs the respiratory chain in ROS 17/2.8 osteoblastic cells. *PLoS One* 9(6):e100768. <https://doi.org/10.1371/journal.pone-0100768>
45. Suzuki M, Bandoski C, Bartlett JD (2015) Fluoride induces oxidative damage and SIRT1/autophagy through ROS-mediated JNK signaling. *Free Radic Biol Med* 89:369–378. <https://doi.org/10.1016/j.freeradbiomed.2015.08.015>
46. Wang S, Deng Z, Ma Y, Jin J, Qi F, Li S, Liu C, Lyu FJ, Zheng Q (2020) The role of autophagy and mitophagy in bone metabolic disorders. *Int J Biol Sci* 16(14):2675–2691. <https://doi.org/10.7150/ijbs-46627>
47. Gu X, Wang Z, Gao J, Han D, Zhang L, Chen P, Luo G, Han B (2019) SIRT1 suppresses p53-dependent apoptosis by modulation of p21 in osteoblast-like MC3T3-E1 cells exposed to fluoride. *Toxicol In Vitro* 57:28–38. <https://doi.org/10.1016/j.tiv-2019-02-006>
48. Li R, Gong Z, Yu Y, Niu R, Bian S, Sun Z (2022) Alleviative effects of exercise on bone remodeling in fluorosis mice. *Biol Trace Elem Res* 200(3):1248–1261. <https://doi.org/10.1007/s12011-021-02741-y>

Publisher's Note Springer Nature remains neutral with regard to jurisdictional claims in published maps and institutional affiliations.

Springer Nature or its licensor holds exclusive rights to this article under a publishing agreement with the author(s) or other rightsholder(s); author self-archiving of the accepted manuscript version of this article is solely governed by the terms of such publishing agreement and applicable law.